Original Article

Avicenna Journal of Medical Biotechnology
Volume 14, Issue no. 3, 247-258
https://doi.org/10.18502/ajmb.v14i3.9832

Check for updates

An *in silico* Design, Expression and Purification of a Chimeric Protein as an Immunogen Candidate Consisting of IpaD, StxB, and TolC Proteins from *Shigella* spp.

Javad Fathi [1,2], Shahram Nazarian [3*], Emad Kordbacheh [3], and Nahal Hadi [1*]

1. Department of Bacteriology and Virology, Faculty of Medicine, Shiraz University of Medical Sciences, Shiraz, Iran
2. Student Research Committee, Faculty of Medicine, Shiraz University of Medical Sciences, Shiraz, Iran
3. Department of Biological Sciences, Faculty of Science, Imam Hossein University, Tehran, Iran

Abstract

Background: *Shigella* spp. is the cause of dysentery and is widespread worldwide. On the other hand, antibiotic resistance is increasing in this bacterium. Bioinformatics is a new approach to vaccine and drug design involving the selection of appropriate antigens. This study aimed to design a chimeric protein consisting of IpaD, StxB, and TolC proteins from *Shigella* through a bioinformatics approach as an immunogen candidate.

Methods: The sequences of *ipaD*, *stxB*, and *tolC* genes were obtained. Additionally, the immunogenic regions of the associated protein, physicochemical characteristics, protein structures, B and T cells epitopes, and molecular docking were determined using *in silico* servers. Besides, the chimeric gene was synthesized following sequence optimization by utilizing the codon usage of *Escherichia coli* (*E. coli*). The expression of the recombinant protein was confirmed *via* SDS-PAGE and Western blot technique.

Results: The residues 41-160 of IpaD, 21-89 of StxB, and 40-335 of TolC were selected. According to half-life, instability, and buried indices, IpaD-StxB-TolC was selected as the best arrangement. The Ramachandran plot showed that 97.077% of the amino acids were in the favored area. Linear and conformational epitopes were also present throughout the chimeric protein sequence. Moreover, the C-ImmSim server indicated that IgG and IgM titers could reach desirable values by the third injection .Furthermore, the stability of the mRNA-optimized gene was enhanced, increasing the Codon Adaptive Index (CAI) to 0.9. Finally, the chimeric gene was transferred to *E. coli* BL21, and the expression of the 60.6 *kDa* recombinant protein was confirmed.

Conclusion: The results indicated that the recombinant protein could act as a proper immunogen candidate against *Shigella* spp.

Avicenna J Med Biotech 2022; 14(3): 247-258

Keywords: Computer simulation, Dysentery, Recombinant fusion proteins, *Shigella* spp, Shigella vaccine candidate

*** Corresponding authors:**
Nahal Hadi, Ph.D., Department of Bacteriology and Virology, School of Medicine, Shiraz University of Medical Sciences, Shiraz, Iran

Shahram Nazarian, Ph.D., Department of Biological Sciences, Faculty of Science, Imam Hossein University, Tehran, Iran
Tel: +98 713 2305884 (Ext: 4544)
E-mail: nahalhadi@gmail.com, nazarian56@gmail.com
Received: 4 Dec 2021
Accepted: 30 Jan 2022

Introduction

Diarrheal diseases are the leading cause of death amongst children in developing countries. These diseases are also the second leading cause of death worldwide after respiratory diseases. The Enterobacteriaceae family is one of the most important causes of these diseases [1,2]. *Shigella* is one of the main causes of gastrointestinal diseases and diarrhea in this family and includes four species, namely *Shigella boydii*, *Shigella dysenteriae*, *Shigella flexneri (S. flexneri), and Shigella sonnei*. Diarrhea caused by *Shigella* can be a simple watery or dysentery (bloody) diarrhea. Diarrhea caused by *Shigella* is also known as Shigellosis and is mainly common in developing countries with poor health and dense populations [3,4]. According to the latest studies, 80 million dysentery cases and more than 700,000 associated deaths are reported annually [5,6].

Shigella contains various virulence factors (binding and invasion factors) and toxins, which are considered pathogens causing infection and death [7]. Among its invasion factors, TolC protein plays an important role in binding of bacteria to host cells, secretion of bacterial toxins, and excretion of antibiotics from bacteria. This protein can create a water-filled channel across the inner and outer membranes, leading molecules to secret from the bacteria without entering the periplasmic space. Therefore, the TolC plays a critical role in

Copyright © 2022, Avicenna Journal of Medical Biotechnology. All rights reserved.

increasing multidrug resistance and is important for the survival of pathogenic bacteria during infection [8,9]. Another virulence factor contains Invasive plasmid antigens (Ipa) that enter the host cell through the Type III Secretion System (T3SS) [10]. These proteins include IpaA, IpaB, IpaC, and IpaD, the last of which controls T3SS secretion, phagosome escape, and macrophage apoptosis. The IpaD is located at the tip of the T3SS apparatus by IpaB, which leads to the bacteria-host cell binding and invading. Due to the IpaD location at the tip of the T3SS and its conservation among *Shigella* serotypes, it has been recognized as a candidate antigen for inducing immune system response [11,12]. Following the binding and colonization of bacteria in the intestine, Shiga toxin (Stx) is produced. This toxin inhibits protein synthesis, thus causing ulcers in intestinal cells [13]. The Stx consists of two subunits, A and B. The A subunit is linked non-covalently to five identical B subunits. The role of the subunit B is to bind, create pores, and enter endothelial cells, while the subunit A has an enzymatic function and leads to the inhibition of protein synthesis and apoptosis in host cells [14,15].

Antibiotics are one of the important strategies for preventing the spread and treatment of Shigellosis, leading to the improvement of health conditions [16]. However, due to the increasing and irregular use of antibiotics, antibiotic resistance is emerging. In the recent decades, the production of ESBL and AmpC beta-lactamases in *Shigella* spp. has increased worldwide. Hence, the production of various forms of these enzymes can be considered the main mechanism of resistance against beta-lactam agents; *i.e.*, cephalosporins. This mechanism can reduce the efficacy of treatment strategies used to cure Shigellosis [17]. In addition, various strategies have been used for decades for making safe and effective vaccines against *Shigella* spp., but a licensed, safe, and well-functioning vaccine is not available yet. One of the novel ways to produce a vaccine against *Shigella* is chimeric protein vaccines. These polyvalent vaccines can reduce the cost of producing and injecting vaccines [18,19]. Chimeric proteins carrying effective epitopes or adjuvant sequences increase the possibility of eliciting a broad cellular or humoral immune response [20,21].

Today, a new field of science so-called bioinformatics has been developed with the evolution of computer science and information technology and the ability to analyze biological data as well as the sequencing of genomes and proteins [22-28]. Immunoinformatic approaches can be used in various fields including prediction of B and T cell epitopes, immune response simulations, antigen receptor interaction, *etc*. Utilization of computational methods can reduce the time and cost of experimental phase in various medical-diagnostic fields [29]. Therefore, the present study aims to design a chimeric protein consisting of IpaD, StxB, and TolC proteins from *Shigella* spp. through a bioinformatics approach as an immunogen candidate.

Materials and Methods

Retrieval of antigen and cassette design

Initially, the amino acid sequences of StxB (UniProt entry: Q7BQ98), IpaD (UniProt entry: P18013), and TolC (UniProt entry: P0AAX2) proteins were obtained from an online database (www.uniprot.org) and were saved in FASTA format. Then, to determine the conserved domains and antigenic segment, the Clustal Omega server (https://www.ebi.ac.uk/Tools/msa/clustalo/) was used as provided by the EBI database (https://www.ebi.ac.uk/Tools/msa/clustalo/). The related sequences for designing the chimeric construct were StxB (accession No. EF685161.1), IpaD (accession No. GQ201921.1), and TolC (accession No. X00016). To maintain the structural stability of the chimeric protein and non-interference of domains, rigid linkers (EAAAK) including glutamic acid, alanine, and lysine were applied. The 6-XHis sequence was also embedded to the C-terminal of the recombinant protein to achieve protein purification and identification.

The physicochemical characteristics of the construct In this step, construct properties were evaluated using the ExPASy ProtParam tool (http://us.expasy.org/tools/protparam.html). These features included the physicochemical properties, molecular weight, theoretical isoelectric point (pI), instability index, extinction coefficient, half-life, aliphatic index, Grand Average Hydropathy (GRAVY), and the total number of positive and negative residues [30].

Prediction of the secondary structure

PHD (http://npsa-pbil.ibcp.fr/cgi-bin/npsa) [31], PORTER (http://distill.ucd.ie/porter/) [32], GORV (http://gor.bb.iastate.edu/) [33], SOPMA (http://npsapbil. ibcp.fr/cgi-bin/npsa) [34], and PREDATOR (http://npsa-pbil.ibcp.fr/cgi-bin/npsa) [35] online servers were used to determine and predict the second structure.

Prediction of the 3D structure

I-TASSER server (http://zhanglab.ccmb.med.umich.edu/I-TASSER/) was used to predict the three-dimensional structure and to determine the best order of the StxB, IpaD, and TolC sections in the chimeric protein. Finally, the predicted PDB file was used as the conformational structures for further evaluations [36].

Tertiary structure refinement

Using the UCSF Chimera v1.15, the best predicted model for chimera was viewed and assessed for topology errors [37]. Afterwards, the 3Drefine and GalaxyWEB servers (http://galaxy.seoklab. org/cgi-bin/submit.cgi?type=REFINE) were used to refine the best obtained model [38,39]. Atomic-level energy minimization and optimization of the hydrogen bonding network so-called MESHI force fields were performed by the i3Drefine refinement algorithm. The GalaxyRefine server was also used to promote the quality of local and global structures *via* side-chain repacking using the molecular dynamics simulation method.

Validation of the 3D structure model

In order to appraise the progress of crystallographic model building and refining, ERRAT server (http://services.mbi.ucla.edu/ERRAT/) was used as a protein structure authentication algorithm. Ramachandran plot and ProSA web server were also utilized for further confirmation of the predicted 3D structure. Finally, NetSurfP server (http://www.cbs.dtu.dk/services/NetSurfP/) and Oklahoma University web-based service (http://www.biotech.ou.edu/) were used to determine the surface residues in the recombinant protein as well as the protein solubility according to the final produced and refined model.

Validation of structural quality

Some indices like Root Mean Square Deviation (RMSD) and TM-score were employed to verify the 3D morphology of the predicted models. They were presented by the predictor servers. Furthermore, to distinguish the errors of the best predicted model, its 3D format (PDB) was uploaded in ProSA and SAVES v5.0 web services [40,41]. The quality of the stereochemistry results was also investigated in the Ramachandran plot in the RAMPAGE server [42].

Protein structures

Firstly, the amino acid composition was analyzed using the protein predictor server for disulfide bonds [43]. The GOR and PHD methods were utilized for homology modeling of the secondary structure consisting of alpha helices and beta sheets. Hence, the PSIPRED and scratch protein predictor servers were operated in these terms as well as in the prediction of solvent accessibility [44,45]. For generating a validated tertiary structure, *ab initio* and comparative modeling algorithms are customary. Based on experience, the RaptorX (http://raptorx.uchicago.edu/StructurePropertyPred/predict/) and the Iterative Threading Assembly Refinement (I-TASSER) servers (https://zhanggroup.org/I-TASSER/) are more reliable. Thus, they were exploited [46,47]. Finally, the DOG 1.0 program was used to visualize the produced 3D models [48].

Molecular docking

Molecular docking is a good approach to drug design. According to the literature, the Stx has an interaction with the Gb3 protein receptor. Hence, the best crystal structures with the lowest resolution of the Gb3 receptor were retrieved from the RCSB database (A.n 1D1K), and docking was done following the removal of H2O, heteroatoms, and unrelated residues and the addition of polar hydrogens. In addition, the structure of the receptor protein was prepared with the help of the PyMOL software. Moreover, ClusPro v2.0 and HADDOCK servers were used to simulate the receptor-ligand docking [49,50]. The ClusPro can rotate ligand and receptor proteins around each other. This program performs a rigid docking by utilizing Fast Fourier Transform (FFT) methods named PIPER. Subsequently, the server scores probable docked structures with the lowest energy and stable cluster size based on the Semi-Definite programming-based Underestimation (SDU) algorithm and Monte-Carlo simulation refinement. In the present study, High Ambiguity Driven protein-protein Docking (HADDOCK) 2.4 server was employed using a flexible docking approach. HADDOCK uses a group of python scripts that use Nuclear Magnetic Resonance (NMR) and crystallography data plus ab-initio docking. This server performs modeling based on Optimized Potentials for Liquid Simulations (OPLS) force field in three steps; *i.e.*, rigid-body energy minimization, semi-flexible refinement, and final refinement. Then, best docking proteins were submitted to the PRODIGY server (PROtein binDIng enerGY prediction) to obtain free energy (ΔG) and dissociation constant (Kd) data and were finally visualized in the PyMOL v.2.3 software [51]. After docking, the complex structure of the designed candidate vaccine with the Gb3 receptor was analyzed by iMOD and CABSflex servers to determine the stability and mobility of the complexes.

B and T cells epitopes

At this stage, B-cell linear epitopes with various lengths were investigated using the Bcepred server [52]. Non-linear B-cell epitopes were also evaluated using CBTOPE, which could predict conformational epitopes by the first protein structure or sequence [53]. The residues overlap was considered using the IEDB server to determine the T cell epitope competence [54]. For the chosen peptides, Cytotoxic T Lymphocytes (CTL) and Helper T Lymphocytes (HTL) epitopes were identified. Therefore, Major Histocompatibility Complex (MHC)-I and MHC-II epitopes were predicted for human alleles. Finally, the full Human Leukocyte Antigen (HLA), the best supertypes of MHC-I, and a high overall score for MHC-II peptides were chosen. According to the IEDB recommended value with a word length of 16 residues, the binding affinity of the MHC molecules and the half-maximal inhibitory concentration (IC50) cut-off of the HTL epitopes were set.

Sequence optimization and mRNA structure prediction

RNA Predict Secondary Structure Server and Vienna RNA Web Servers (RNAfold) were used to investigate the chimeric gene parameters as well as the mRNA secondary structure [55,56]. The sequence optimization was performed for high-level expression in *Escherichia coli* (*E. coli*). The RNA secondary structure was compared before and after codon optimization. The minimum energies of the native and optimized mRNA were compared, as well [57].

Immune simulation

C-ImmSim server (https://www.iac.rm.cnr.it/~filippo/projects/c-immsim-online.html) was used to predict the *in silico* immune response profile of the chimeric protein. This server could describe the humoral and cellular immune responses against the recombinant protein. Finally, three administrations were set with

four-week intervals.

Expression, verification, and purification of the recombinant chimeric protein

After designing and ordering the chimeric IpaD-StxB-TolC gene in pET28a (ShineGene, China), this structure was transferred to *E. coli* BL21 (DE3) by the heat shock method. Then, by adding 1 *mM* isopropyl-β-d-thiogalactoside (IPTG; Sigma, USA) to the bacterial culture medium, recombinant protein production was induced and incubated at 37℃ for 5 *hr*. After that, the culture medium was centrifuged (5000×*g* at 25℃ for 10 *min*) and the bacterial precipitate was mixed with the lysis buffer (100 *mM* NaH_2PO_4, 10 *mM* Tris-HCl, 8 *M* urea, pH=8.0). In the next step, after sonication (6 times for 10 *s* with high power), the lysed cell was centrifuged at 10000 *g* at 4℃ for 15 *min*, the precipitate was discarded, and the supernatant was loaded in the Ni-NTA chromatography column (Qiagen). Protein elution was achieved using the elution buffer containing 100 *mM* NaH_2PO_4, 10 *mM* Tris-base, and 8 *M* urea (pH=4.2). SDS PAGE 10% and Western blot analysis using anti-His tag antibody were performed to confirm the recombinant protein expression.

Results

Sequence arrangement and physicochemical characteristics of the construct

StxB, IpaD, and TolC proteins were selected as acceptable immunogens and immunogen candidates based on the previous studies. Protein sequences of StxB, IpaD, and TolC were retrieved from the Uniprot database and were aligned with the Clustal omega server. To design the recombinant protein, residues 41-160 of IpaD, 21-89 of StxB (without the signal peptide), and 40-335 of TolC were selected. Three repeats of EAAAK (as a rigid linker) were also placed among the recombinant protein subunits to maintain the structure and independent function of each protein subunit (Figure 1). Finally, in order to achieve protein purification and identification, the 6-XHis sequence was embedded to the recombinant proteins C-terminal. For the best arrangement, several factors including half-life, instability index (https://web.expasy.org/protparam/), VaxiJen score (http://www.ddg-pharmfac.net/vaxijen/VaxiJen/VaxiJen.html), solvent access (http://raptorx.uchicago.edu/StructurePropertyPred/predict/), protein solubility (https://proteinsol.manchester. ac.uk/), and allergencity evidence (https://www.ddgpharmfac.net/AllerTOP/index.html) were evaluated (Table 1). According to half-life, instability, and buried indices, IpaD-StxB-TolC was selected as the best arrangement for the desired cassette.

Prediction of the structures

The second structure was evaluated using GORIV, and the third structure (Figure 2) was built *via* I-TASSER, RaptorX, and Phyre2 model (Table 2). After that, the most morphologically favorable and stable models were selected. The quality of the predicted structure was evaluated using the Ramachandran plot and the PROSA software (Figure 3).

Molecular docking and dynamic simulations

The docking of the structure of the designed candidate vaccine with Gb3 by the ClusPro server led to the

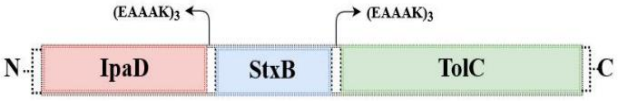

Figure 1. Schematic presentation of the recombinant protein construct consisting of StxB, IpaD, and TolC proteins bound together by the EAAAK linkers.

Table 1. Determining the best arrangement and the physicochemical characteristics

Arrangement	Half-life	Instability index	VaxiJen score	Solvent access *	Protein solubility	*Allergenicity* evidence
IpaD-StxB-TolC	100 *hr* (mammalian reticulocytes, *in vitro*) >20 *hr* (yeast, *in vivo*) >10 *hr* (Escherichia coli, *in vivo*)	28.69	0.6254	50% E 30% M 18% B	Soluble	0.0%
IpaD-TolC-StxB	100 *hr* (mammalian reticulocytes, *in vitro*) >20 *hr* (yeast, *in vivo*) >10 *hr* (Escherichia coli, *in vivo*)	29.06	0.6327	49% E 31% M 19% B	Soluble	0.0%
StxB-TolC-IpaD	7.2 *hr* (mammalian reticulocytes, *in vitro*) >20 *hr* (yeast, *in vivo*) >10 *hr* (escherichia coli, *in vivo*)	29.04	0.6293	48% E 32% M 19% B	Soluble	0.0%
StxB-IpaD-TolC	7.2 *hr* (mammalian reticulocytes, *in vitro*) >20 *hr* (yeast, *in vivo*) >10 *hr* (escherichia coli, *in vivo*)	28.52	0.6269	48% E 30% M 20% B	Soluble	0.0%
TolC-StxB-IpaD	1 *hr* (mammalian reticulocytes, *in vitro*) 2 *min* (yeast, *in vivo*) 2 *min* (escherichia coli, *in vivo*)	28.41	0.6258	47% E 34% M 18% B	Soluble	0.0%
TolC-IpaD-StxB	1 *hr* (mammalian reticulocytes, *in vitro*) 2 *min* (yeast, *in vivo*) 2 *min* (escherichia coli, *in vivo*)	28.27	0.6308	48% E 32% M 19% B	Soluble	0.0%

* E: Exposure, M: Mediate, B: Buried.

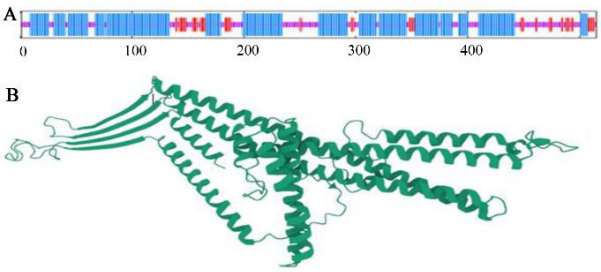

Figure 2. Graphical presentation and assessment of the secondary structure (A). Cartooned secondary structure showing helix 61%, strands 11%, coils 26%, and 50% exposure. Concerning the tertiary structure, the RaptorX predicted the lack of a major burial domain (18%), as shown by the UCSF Chimera (B).

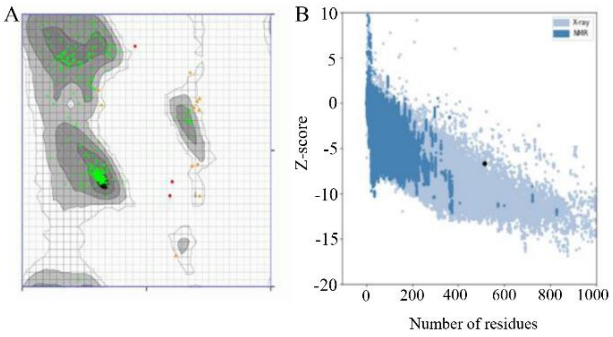

Figure 3. As the Ramachandran plot views the error values of the residues, 97.077% of the amino acids were in the favored area (A). Z-score plots of the ProSA server compared the subunit protein to the pre-determined X-ray and NMR structures and confirmed the angle and distance of the residues (B).

generation of 10 models. The flexible dock was predicted by the HADDOCK server. The receptor protein had interactions with the Stx regions of the protein. Regarding ClusPro, based on the lowest energy scores (-1042.2 *kJ/mol*), model number 0 was selected for the Gb3-candidate vaccine complex as the best-docked complex with ΔG of -18.3 (*kcal mol*$^{-1}$) by PRODIGY. The HADDOCK server predicted 81 structures in 15 clusters, with the best cluster presenting a score of 97.5±8.0 and ΔG of -16.6 (*kcal mol*$^{-1}$) at 37.0℃. Moreover, the LigPlot analysis indicated that the receptor-protein complex included salt bridges, hydrogen bonds, and non-bonded contacts (Figure 4A). CABSflex and iMOD servers performed the molecular dynamic simulation of the protein receptor interaction. As shown in figure 4B, B-factor mode presentation of the complex showed less deviation in atomic fluctuation. Consequently, it was a solid interaction. Besides, the eigenvalue of the protein-receptor was 4.577188e-6, which implied its stability.

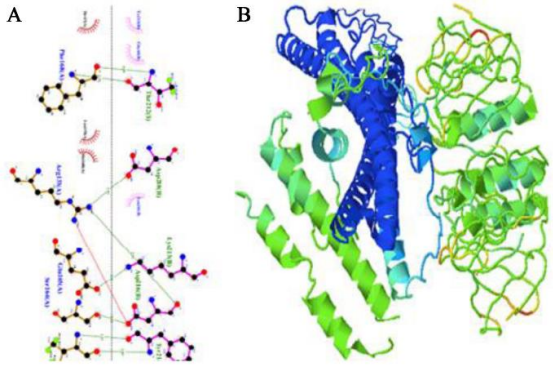

Figure 4. Molecular docking and dynamic simulations. A) the receptor-protein complex, B) the molecular dynamic simulation of the protein receptor interaction.

Prediction of B cell epitope

Vaccine candidates should be able to induce the response of both B and T cells. Determination of B linear epitopes is possible using their innate affinity for amino acids and bioinformatics algorithms. The linear epitopes of B cells in the chimeric protein predicted by the BCpred server have been depicted in figure 5. Accordingly, the linear epitopes were present throughout the chimeric protein sequence and belonged to three subunits (IpaD-StxB-TolC) of this protein. The results of predicting the conformational B-cell epitopes using CBTOPE and Discotope servers have been presented in table 3. Based on the results, conformational B-cell epitopes were present throughout the recombinant pro tein sequence and belonged to the three abovementioned proteins.

Prediction of T cell epitopes

The MHC-I and MHC-II binding prediction tools from the IEDB server were employed to investigate T-cell epitopes (Table 4). According to the results, five most frequent alleles in eight residue lengths were chosen for MHC class I. Additionally, five most frequent alleles in 14 residue lengths were selected for MHC-II.

Immune simulation

Generally, the C-ImmSim can be successfully used to determine immune responses. As illustrated in figure 6, recognition of the subunit protein and the proper

Table 2. The third structures predicted by different tools and comparison of their scores

Model name	ERRAT	Veryfy3d	Ramachandran plot statistics		
			Most favored regions	Allowed regions	Disallowed regions
I-TA SSER model	91.1828	47.57%	88.309%	7.516%	7.516%
RaptorX model	88.8224	32.62%	97.077%	2.296%	0.626%
Phyre2 model	87.0849	27.69%	96.085%	2.135%	1.779%

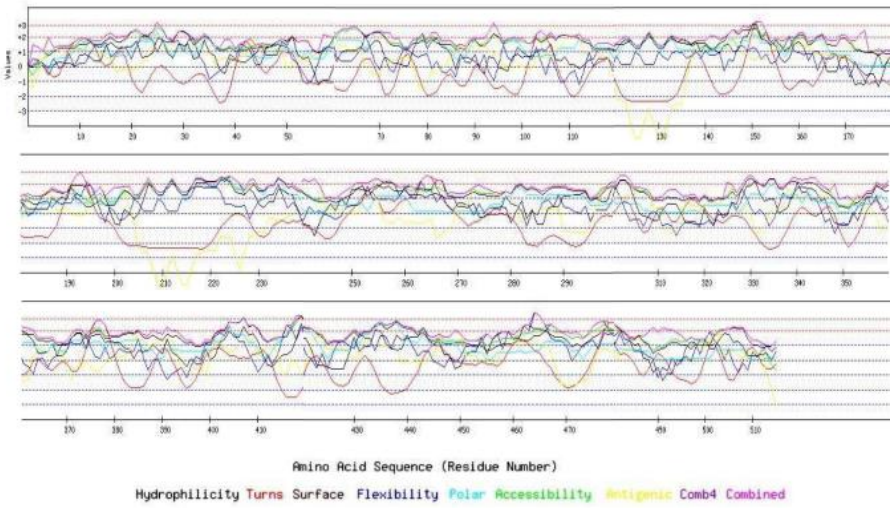

Figure 5. B-cell epitopes from IpaD-StxB-TolC full-length proteins using the BCpred server.

Table 3. Conformational B-cell epitopes from full-length IpaD-StxB-TolC protein using the CBTOPE and discotope servers

CBTOPE			Discotope										
Amino acid	**Position**	**Score**	**Amino acid**	**Position**	**Contact number**	**Score**	**Amino acid**	**Position**	**Contact number**	**Score**	**Amino acid**	**Position**	**Contact number**	**Score**
KDARELLHSA	67-77	4	SER	3	-3.638	-3.220	SER	42	-1.343	-3.259	GLY	261	3.417	2.909
DCVTGK	137-143	4	ASN	8	-3.062	-3.285	LYS	46	-2.486	-3.350	ASP	279	2.071	-3.444
TIKTNACHNG	185-195	6	HIS	12	-3.401	-3.585	SER	53	-2.241	-3.594	LEU	288	3.609	-3.168
IFRE	201-205	4	ARG	15	-2.389	-2.689	ASP	57	-1.846	-3.259	ASP	297	-2.997	-3.686
ARSPLLPQL	235-244	4	ASN	18	-1.163	-1.834	GLU	63	-2.754	-3.587	ASN	402	-2.303	-2.959
YTYSNGYRDAN	249-260	5	GLN	19	-0.734	-1.221	LYS	68	-3.227	-2.856	PRO	410	-2.303	-3.653
YTYSNGYRDAN	266-273	4	ALA	20	-1.306	-2.536	GLU	72	-3.606	-3.534	LEU	415	-3.505	-3.448
KAAGIQDVTYQTD	290-303	4	LEU	21	1.101	-3.505	VAL	144	-2.080	-2.416	GLU	435	-1.797	-3.549
DQTTQRFNVGLVA ITDVQNARA-QYDTVLANEV	339-371	4	LYS	22	-0.508	-1.207	GLU	145	-2.466	-2.988	ALA	442	-0.506	-2.930
EQLRQITGNYYPEL AAL-NVENFKTDKPQPV NALL	381-415	4	LYS	23	-0.715	-1.208	TYR	149	-1.014	-2.278	ALA	454	-3.484	-3.428
RQAQDGHL	439-447	4	LEU	25	-1.310	-3.229	ASP	153	-2.599	-3.300	THR	474	4.709	3.503
SKTRGAAGTQYDD SNMGQNKVGLSFS LPIYQGGMVNS-QVKQAQYNFVGAS	465-515	5	LYS	28	-1.236	-3.0164	GLY	539	-1.460	-1.292	GLN	475	4.900	3.761
			THR	31	-1.981	-2.214	PHE	230	-1.851	-3.133	ASP	478	5.006	1.096
			SER	34	-2.563	-3.533	ASN	234	-1.458	-3.474	SER	479	5.028	4.334
			LEU	35	-2.858	-3.104	TYR	252	-2.845	-3.157	VAL	486	-3.472	-3.648
			ILE	38	-1.629	-3.511	TYR	256	4.458	2.244	SER	502	-0.653	-3.107
			HIS	41	-1.095	-3.384	ARG	257	4.517	2.732	GLN	506	-0.524	-2.879

immune response resulted in an increase in antibody titer. In the second injection, the IgG and IgM immunoglobulin titers started to increase, reaching the maximum values in the third injection.

Sequence optimization and mRNA structure prediction

To enhance the transcriptional and translational function of *E. coli*, the sequence encoding the IpaD-StxB-TolC chimeric gene was optimized *via* the optimizer and the rare codon analysis tool. As shown in table 5, the Codon Adaptation Index (CAI) was 0.74 before optimization and 0.90 after that (ideal value = 0.8-1.0). The GC content also increased from 46.45% to 54.63%) ideal value=30-70%).

The thermodynamic properties of the secondary structure of mRNA indicated an increase in the stability of the mRNA optimized gene. The RNA secondary

Table 4. Selection of peptides containing T cell epitopes from the chimeric protein by MHC-I and MHC-II binding prediction algorithms

MHC	Allele	Start	End	Percentile rank	Peptide
I	HLA-A*02:01	6	14	0.02	MLNDTLHNI
I	HLA-B*07:02	407	415	0.03	KPQPVNALL
I	HLA-A*03:01	20	28	0.03	ALKKDLSQK
I	HLA-A*24:02	299	307	0.04	TYQTDQQTL
I	HLA-A*01:01	455	463	0.08	STGISDTSY
II	HLA-DRB3*02:02	303	317	0.01	DQQTLILNTATAYFN
II	HLA-DRB1*07:01	444	458	0.27	DGHLPTLDLTASTGI
II	HLA-DRB3*01:01	295	309	0.72	IQDVTYQTDQQTLIL
II	HLA-DRB1*03:01	63	77	2.40	EYPINKDARELLHSA
II	HLA-DRB1*15:01	420	434	4.00	KRNLSLLQARLSQDL

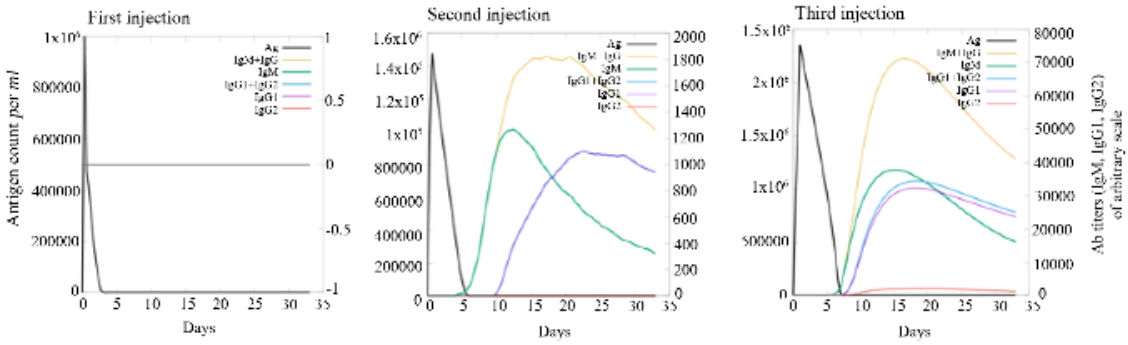

Figure 6. The C-ImmSim immune response simulation immunoglobulins levels after the injections. The hypothetical administration of the vaccine was carried out in three injections given four weeks apart.

Table 5. Sequence optimization

	Before optimization	After optimization	Ideal value
CAI	0.74	0.90	0.8-1.0
GC Content	46.45%	54.63%	30-70%
CFD	6%	0%	<30%
Negative repeat elements	5	0	
Negative CIS elements	0	0	

structure of the chimeric gene was predicted using the Mofld algorithm (Figure 7). The predicted structure did not have stable hairpin and pseudoknot at the 5' site of the mRNA.

Expression, purification, and verification of the chimeric protein

The recombinant vector was transferred to the *E. coli BL21* strain, inducing recombinant protein expression by IPTG. A 60/6 *kDa* protein band on SDS-PAGE 10% showed a high level of recombinant protein expression (Figure 8A). Purification of the protein was carried out by Ni-NTA chromatography column and under native conditions. SDS-PAGE 10% analysis revealed the presence of the recombinant protein in the eluted fraction (IM 250) (Figure 8B). Finally, the recombinant protein was confirmed by western blot using an anti-His tag antibody (Figure 9).

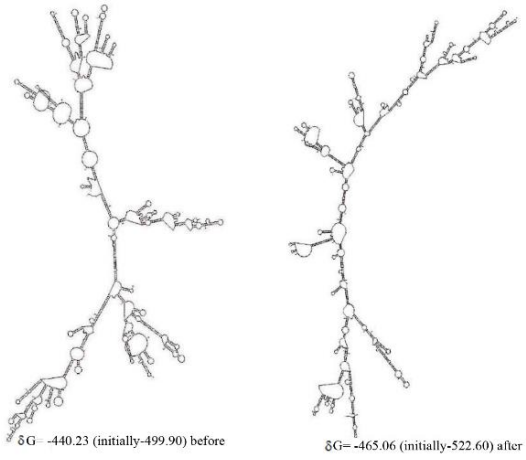

Figure 7. Prediction of the RNA secondary structure of the chimeric gene using the Mofld algorithm.

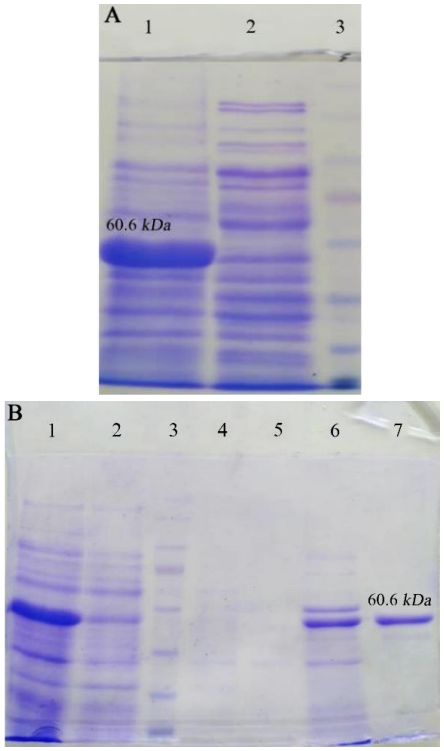

Figure 8. A) Expression of the recombinant protein. Lane 1: Expression of the recombinant protein induced by IPTG. Lane 2: Expression of the recombinant protein without IPTG. Lane 3: Protein weight marker (prestained protein ladder, 10-170 *kDa*). B) SDS-PAGE 10% of the chimeric protein (IpaD-StxB-TolC). Lane 1: Cell lysate *E. coli* containing pET28a induced by IPTG. Lane 2: Flow-through. Lane 3: Protein weight marker (prestained protein ladder, 10-170 *kDa*). Lane 4: Wash C fraction (pH=6.3). Lane 5: Wash D fraction (pH=5.9). Lane 6: Wash E fraction (pH=4.3). Lane 7: Elution fraction (IM 250).

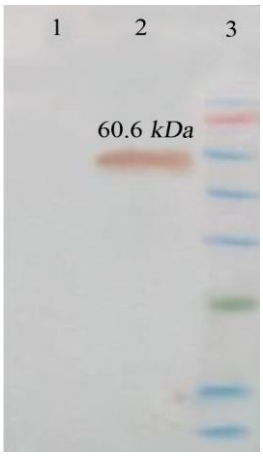

Figure 9. Identification of protein expression (IpaD-StxB-TolC) using western blot analysis. The anti-His antibody detected the expression of a chimeric protein (60.6 *kDa*). Lane 1: Control (Bovine Serum Albumin, BSA). Lane 2: Chimeric protein. Lane 3: Protein weight marker (prestained protein ladder, 10- 170 *kDa*).

Discussion

Shigella spp. are intracellular pathogenic bacteria that colonize the gastrointestinal tract, especially intestinal cells, and cause bacillary dysentery by invading these cells. Bacillary dysentery has been a problem in developing countries, mainly causing symptoms and diseases in children, immunocompromised patients, and elderly individuals [58]. Invasion and pathogenicity of *Shigella* are increased through the secretion system, binding, invasion factors, bacterial toxins, and excretion of antibiotics from bacteria. *Shigella*, as an intracellular pathogen, has challenged antibiotic treatment approaches. Although fluoroquinolones, cephalosporins, and azithromycin are used to treat *Shigella*, resistance to these antibiotics is growing, which is a major concern in treating this bacterium [59]. Designing effective vaccines against *Shigella* can be a good way to overcome antibiotic resistance as well as to control and prevent the spread of this bacterium [60]. Although most live vaccines can provide better protection against pathogens compared to other vaccines, the attenuation process and achievement of minimum toxicity is a difficult process. On the other hand, due to the induction of immunosuppressive conditions, the use of live *Shigella* vaccines can interfere with the immune response of the host and cause immune reactions [61,62]. Recombinant and subunit vaccines are a new and effective strategy against pathogens such as *Shigella*. The use of several different antigens in a chimeric protein can induce and produce several antibodies simultaneously against the pathogen [63]. IpaD is a highly conserved protein among *Shigella* serotypes and is located at the tip of the T3SS. The role of this protein is to bind and invade bacteria to host cells [11]. Previous studies have proved that the IpaD has the ability to stimulate the immune system and produce antibodies. Thus, any mutation or deletion in this protein leads to defects in bacterial functions including secretion control and insertion of translocators into host cell membranes [12,64]. *S. dysentery* secretes Stx toxin, which binds to host ribosomes and results in the apoptotic death of host cells by inhibiting protein synthesis [13,65]. The StxB subunit binds to the host cell, while the StxA subunit plays an enzymatic role and inhibits protein synthesis. The previous studies have also emphasized that StxB has an adjuvant role in addition to the ability to induce antibody production [14,66,67]. Furthermore, numerous studies have reported that the outer membrane channel protein (TolC) is involved in multidrug resistance in gram-negative bacteria including *S. flexneri*. TolC is also involved in the binding of bacteria to host cells, secretion of bacterial toxins, and excretion of antibiotics from bacteria [8,68].

Nowadays, bioinformatics tools and approaches can help design chimeric proteins and vaccine candidates. Thus, online bioinformatics tools were utilized in the current investigation to design a vaccine candidate against *Shigella* spp. based on B and T cells epitopes and production of antibodies (IgG and IgM). Considering the increasing antibiotic resistance, lack of an effective vaccine against *Shigella* spp., and advantages of

bioinformatics, this study aimed to design a chimeric protein consisting of IpaD, StxB, and TolC proteins from *Shigella* through a bioinformatics approach as an immunogen candidate. In this study, the protein sequences of IpaD, StxB, and TolC were retrieved from the Uniprot database and were aligned with the Clustal omega server. Residues 41-160 of IpaD, 21-89 of StxB (without the signal peptide), and 40-335 of TolC were selected. Based on the researchers' past experience, Kordbacheh *et al* and Felegary *et al* the selected regions were fused *via* the EAAAK linker and a novel construct was built [69,70]. The EAAAK rigid linker is appropriate for bifunctional chimeric protein. Based on half-life, instability, and buried indices, IpaD-StxB-TolC was found to be the best arrangement. The molecular weight of the chimeric protein was 60.6 *kDa*. The second structure was evaluated via GORIV, and the third structure was built based on the RaptorX model. Accordingly, Helix 61%, strands 11%, coils 26%, and the lack of a major burial domain (18%) were determined. The structure quality was evaluated by the Ramachandran plot and the PROSA software. Based on the findings, 97.077% of the amino acids were in the favored area. Additionally, the Z-score plots determined X-ray and NMR structures and confirmed the angles and distances of the residues. Docking of the vaccine candidate with Gb3 (receptor of StxB) led to the generation of 10 models. Model number 0 with lowest energy scores (-1042.2 *kJ/mol*) was selected for the Gb3-candidate vaccine complex as the best-docked complex with ΔG of -18.3 ($kcal\ mol^{-1}$). Moreover, the HADDOCK server predicted 81 structures in 15 clusters, with the best cluster showing a score of 97.5±8.0 and ΔG of -16.6 ($kcal\ mol^{-1}$) at 37.0 ℃. Besides, the receptor-protein complex included salt bridges, hydrogen bonds, and non-bonded contacts. Molecular dynamic simulation of the protein receptor interaction indicated that the B-factor mode presentation of the complex had less deviation in atomic fluctuation. Consequently, it was a solid interaction. The eigenvalue of the protein-receptor was also 4.577188e-6, implying its stability.

Since vaccines should be able to maximally stimulate the immune system especially B and T cells, and determination of epitopes has a fundamental role in vaccine design, the BCpred server was used to determine the linear B-cell epitopes and CBTOPE and Discotope servers were utilized for predicting the conformational B-cell epitopes. The results revealed that linear and conformational B-cell epitopes were present throughout the chimeric protein sequence and belonged to three subunits (IpaD-StxB-TolC). Furthermore, the IEDB server was used for the prediction of T cell epitopes, which showed five alleles in eight residue lengths for MHC-I and five alleles in 14 residue lengths for MHC-II. Assessment of the immune responses and production of antibodies against the chimeric protein through C-ImmSim indicated that the highest IgG and IgM titers were obtained after the third injection. After optimizing the sequence encoding the chimeric protein, CAI and GC content increased to 0.90 and 54.63%, respectively and led to an increase in transcription and translation in *E. coli*. The stability of the mRNA optimized gene was enhanced, as well. Additionally, the predicted mRNA structure had no long stable hairpin and pseudoknot at the 5' site. In the last step, after bioinformatics studies and preparation of the recombinant vector, this vector was transferred to *E. coli* BL21 strain. After inducing the bacteria for the expression of the recombinant protein, protein expression was assessed by the SDS-PAGE method and protein confirmation was performed via western blot using anti-His tag antibody. These two methods confirmed the presence of the chimeric protein with the molecular weight of 60.6 *kDa*. In the continuation of this study, this recombinant protein can be evaluated for antibody production and immunogenicity both *in vitro* and *in vivo*.

Conclusion

Shigella spp. is emerging as a global problem due to deadly diseases as well as increased antibiotic resistance. In this context, the lack of an effective vaccine against *Shigella* is a red alert for public health. Today, the use of bioinformatics software has led to more effective and faster studies in vaccine development. In the current research, toxin, T3SS, and binding factors of *Shigella* spp., as a vaccine candidate, were evaluated with the help of bioinformatics software. The findings indicated that the chimeric protein containing IpaD-StxB-TolC had a high ability to stimulate the immune system and, as a vaccine candidate, could lead to immunogenicity and antibody production.

Acknowledgement

The authors would like to thank Ms. A. Keivanshekouh at the Research Consultation Center (RCC) of Shiraz University of Medical Sciences for improving the use of English in the manuscript.

Conflict of Interest

The authors declare no conflict of interests.

Funding: This work was supported by Shiraz University of Medical Sciences, Shiraz, Iran (IR.SUMS.REC.1400.347). It was done based on the results of the PhD dissertation written by Javad Fathi under the supervision of Dr. Nahal Hadi and Dr. Shahram Nazarian.

Data availability statement: The data are available from the corresponding author upon request.

Ethics of Approval Statement

Not applicable.

References

1. Petri WA, Miller M, Binder HJ, Levine MM, Dillingham R, Guerrant RL. Enteric infections, diarrhea, and their impact on function and development. J Clin Invest 2008; 118(4):1277-90.
2. Vansofla AN, Nazarian S, Kordbache E, Fathi J. An IgG/IgY sandwich-ELISA for the detection of heat-labile enterotoxin B subunit of enterotoxigenic Escherichia coli. Gene Reports 2021;23:101099.
3. Anderson M, Sansonetti PJ, Marteyn BS. Shigella diversity and changing landscape: insights for the twenty-first century. Front Cell Infect Microbiol 2016;6: 45.
4. Ugboko HU, Nwinyi OC, Oranusi SU, Oyewale JO. Childhood diarrhoeal diseases in developing countries. Heliyon 2020;6(4):e03690.
5. Khalil IA, Troeger C, Blacker BF, Rao PC, Brown A, Atherly DE, et al. Morbidity and mortality due to shigella and enterotoxigenic Escherichia coli diarrhoea: the Global Burden of Disease Study 1990-2016. Lancet Infect Dis 2018;18(11):1229-40.
6. Tickell KD, Brander RL, Atlas HE, Pernica JM, Walson JL, Pavlinac PB. Identification and management of Shigella infection in children with diarrhoea: a systematic review and meta-analysis. Lancet Glob Health 2017;5 (12):e1235-e48.
7. Kordbacheh E, Nazarian S, Farhang A. An in silico approach for construction of a chimeric protein, targeting virulence factors of Shigella spp. Int J Computational Biology Drug Design 2018;11(4):310-27.
8. Kazi A, Ismail CMKH, Anthony AA, Chuah C, Leow CH, Lim BH, et al. Designing and evaluation of an antibody-targeted chimeric recombinant vaccine encoding Shigella flexneri outer membrane antigens. Infect Genet Evol 2020;80:104176.
9. Koronakis V, Eswaran J, Hughes C. Structure and function of TolC: the bacterial exit duct for proteins and drugs. Annu Rev Biochem 2004;73(1):467-89.
10. Picking WL, Nishioka H, Hearn PD, Baxter MA, Harrington AT, Blocker A, et al. IpaD of Shigella flexneri is independently required for regulation of Ipa protein secretion and efficient insertion of IpaB and IpaC into host membranes. Infect Immun 2005;73(3):1432-40.
11. Muthuramalingam M, Whittier SK, Picking WL, Picking WD. The Shigella type III secretion system: an overview from top to bottom. Microorganisms 2021;9(2):451.
12. Roehrich AD, Guillossou E, Blocker AJ, Martinez-Argudo I. S higella IpaD has a dual role: signal transduction from the type III secretion system needle tip and intracellular secretion regulation. Mol Microbiol 2013;87 (3):690-706.
13. Fathi J, Ebrahimi F, Nazarian S, Hajizade A, Malekzadegan Y, Abdi A. Production of egg yolk antibody (IgY) against shiga-like toxin (stx) and evaluation of its prophylaxis potency in mice. Microb Pathog 2020;145: 104199.
14. Fathi J, Ebrahimi F, Nazarian S, Tarverdizade Y. Purification of shiga-like toxin from Escherichia coli O157: H7 by a simple method. J Applied Biotechnology Reports 2017;4(4):707-11.
15. Kordbacheh E, Nazarian S, Hajizadeh A, Fasihi-Ramandi M, Fathi J. Recombinant HcpA-EspA-Tir-Stx2B chimeric protein induces immunity against attachment and toxicity of Escherichia coli O157: H7. Microb Pathog 2019;129:176-82.
16. Taheri-Anganeh M, Khatami SH, Jamali Z, Movahedpour A, Ghasemi Y, Savardashtaki A, et al. LytU-SH3b fusion protein as a novel and efficient enzybiotic against methicillin-resistant Staphylococcus aureus. Mol Biol Res Commun 2019;8(4):151-8.
17. Zamanlou S, Ahangarzadeh Rezaee M, Aghazadeh M, Ghotaslou R, Babaie F, Khalili Y. Characterization of integrons, extended-spectrum β-lactamases, AmpC cephalosporinase, quinolone resistance, and molecular typing of Shigella spp. from Iran. Infect Dis (Lond) 2018;50(8):616-24.
18. Nagy G, Emo L, Pál T. Strategies for the development of vaccines conferring broad-spectrum protection. Int J Med Microbiol 2008;298(5-6):379-95.
19. Taheri-Anganeh M, Amiri A, Movahedpour A, Khatami SH, Ghasemi Y, Savardashtaki A, et al. In silico evaluation of PLAC1-fliC as a chimeric vaccine against breast cancer. Iran Biomed J 2020;24(3):173-82.
20. Arianzad SA, Zeinoddini M, Haddadi A, Nazarian S, Sajedi RH. In silico design of chimeric and immunogenic protein-containing IpaB and IpaD as a vaccine candidate against Shigella dysenteriae. Current Proteomics 2020;17 (4):333-41.
21. Taheri-Anganeh M, Savardashtaki A, Vafadar A, Movahedpour A, Shabaninejad Z, Maleksabet A, et al. In silico design and evaluation of PRAME+FliCΔD2D3 as a new breast cancer vaccine candidate. Iran J Med Sci 2021;46(1):52-60.
22. Mehrpour K, Mirzaei SA, Savardashtaki A, Nezafat N, Ghasemi Y. Designing an HCV diagnostic kit for common genotypes of the virus in Iran based on conserved regions of core, NS3-protease, NS4A/B, and NS5A/B antigens: an in silico approach. Biologia 2021;76(1):281-96.
23. Shamakhi A, Kordbacheh E. Immunoinformatic design of an epitope-based immunogen candidate against Bacillus anthracis. Informatics in Medicine Unlocked 2021; 24:100574.
24. Taheri-Anganeh M, Khatami SH, Jamali Z, Savardashtaki A, Ghasemi Y, Mostafavi-Pour Z. In silico analysis of suitable signal peptides for secretion of a recombinant alcohol dehydrogenase with a key role in atorvastatin enzymatic synthesis. Mol Biol Res Commun 2019;8(1): 17-26.
25. Vafadar A, Taheri-Anganeh M, Movahedpour A, Jamali Z, Irajie C, Ghasemi Y, et al. In silico design and evaluation of scFv-CdtB as a novel immunotoxin for breast cancer treatment. Int J Cancer Manag 2020;13(1): e96094.
26. Khatami SH, Taheri-Anganeh M, Arianfar F, Savardashtaki A, Sarkari B, Ghasemi Y, et al. Analyzing signal peptides for secretory production of recombinant diag-

nostic antigen B8/1 from Echinococcus granulosus: an in silico approach. Mol Biol Res Commun 020;9(1):1-10.

27. Tehrani SS, Goodarzi G, Naghizadeh M, Khatami SH, Movahedpour A, Abbasi A, et al. Suitable signal peptides for secretory production of recombinant granulocyte colony stimulating factor in Escherichia coli. Recent Pat Biotechnol 2020;14(4):269-82.
28. Samavarchi Tehrani S, Gharibi S, Movahedpour A, Goodarzi G, Jamali Z, Khatami SH, et al. Design and evaluation of scFv-RTX-A as a novel immunotoxin for breast cancer treatment: an in silico approach. J Immunoassay Immunochem 2021;42(1):19-33.
29. Rapin N, Lund O, Bernaschi M, Castiglione F. Computational immunology meets bioinformatics: the use of prediction tools for molecular binding in the simulation of the immune system. PloS One 2010;5(4): e9862.
30. Yamasaki S, Sato T, Hidaka Y, Ozaki H, Ito H, Hirayama T, et al. Structure-activity relationship of Escherichia coli heat-stable enterotoxin: role of Ala residue at position 14 in toxin-receptor interaction. Bulletin of the Chemical Society of Japan 1990;63(7): 2063-70.
31. Rost B, Yachdav G, Liu J. The predictprotein server. Nucleic Acids Res 2004;32(Web server issue):W321-W6.
32. Walsh I, Baù D, Martin AJ, Mooney C, Vullo A, Pollastri G. Ab initio and template-based prediction of multiclass distance maps by two-dimensional recursive neural networks. BMC Struct Biol 2009;9(1):5.
33. Sen TZ, Jernigan RL, Garnier J, Kloczkowski A. GOR V server for protein secondary structure prediction. Bioinformatics 2005;21(11):2787-8.
34. Geourjon C, Deleage G. SOPMA: significant improvements in protein secondary structure prediction by consensus prediction from multiple alignments. Bioinformatics 1995;11(6):681-4.
35. Frishman D, Argos P. Incorporation of non-local interactions in protein secondary structure prediction from the amino acid sequence. Protein Eng 1996;9 (2):133-42.
36. Zhang Y. I-TASSER server for protein 3D structure prediction. BMC Bioinformatics 2008;9(1):40.
37. Pettersen EF, Goddard TD, Huang CC, Couch GS, Greenblatt DM, Meng EC, et al. UCSF Chimera—a visualization system for exploratory research and analysis. J Comput Chem 2004;25(13):1605-12.
38. Bhattacharya D, Nowotny J, Cao R, Cheng JJNar. 3 Drefine: an interactive web server for efficient protein structure refinement. Nucleic Acids Res 2016;44(W1): W406-W9.
39. Ko J, Park H, Heo L, Seok CJNar. GalaxyWEB server for protein structure prediction and refinement. Nucleic Acids Res 2012;40(Web server issue):W294-W7.
40. Wiederstein M, Sippl MJ. ProSA-web: interactive web service for the recognition of errors in three-dimensional structures of proteins. Nucleic Acids Res 2007;35(Web server issue):W407-W10.
41. Pontius J, Richelle J, Wodak SJJJomb. Deviations from standard atomic volumes as a quality measure for protein crystal structures. J Mol Biol 1996;264(1):121-36.
42. Lovell SC, Davis IW, Arendall WB, de Bakker PI, Word JM, Prisant MG, et al. Structure validation by Cαlpha geometry: phi, psi, Cbeta deviation. Proteins 2003;50(3): 437-50.
43. Ceroni A, Passerini A, Vullo A, Frasconi PJNar. DISULFIND: a disulfide bonding state and cysteine connectivity prediction server. Nucleic Acids Res 2006;34(Web server issue):W177-W81.
44. Yachdav G, Kloppmann E, Kajan L, Hecht M, Goldberg T, Hamp T, et al. PredictProtein—an open resource for online prediction of protein structural and functional features. Nucleic Acids Res 2014;42(Web server issue): W337-W43.
45. Buchan DW, Minneci F, Nugent TC, Bryson K, Jones DT. Scalable web services for the PSIPRED Protein Analysis Workbench. Nucleic Acids Res 2013;41(Web server issue):W349-W57.
46. Källberg M, Wang H, Wang S, Peng J, Wang Z, Lu H, et al. Template-based protein structure modeling using the RaptorX web server. Nat Protoc 2012;7(8):1511-22.
47. Yang J, Yan R, Roy A, Xu D, Poisson J, Zhang Y. The I-TASSER Suite: protein structure and function prediction. Nat Methods 2015;12(1):7-8.
48. Ren J, Wen L, Gao X, Jin C, Xue Y, Yao X. DOG 1.0: illustrator of protein domain structures. Cell Res 2009;19 (2):271-3.
49. Porter KA, Xia B, Beglov D, Bohnuud T, Alam N, Schueler-Furman O, et al. ClusPro PeptiDock: efficient global docking of peptide recognition motifs using FFT. Bioinformatics 2017;33(20):3299-301.
50. Van Zundert G, Rodrigues J, Trellet M, Schmitz C, Kastritis P, Karaca E, et al. The HADDOCK2. 2 web server: user-friendly integrative modeling of biomolecular complexes. J Mol Biol 2016;428(4):720-5.
51. Xue LC, Rodrigues JP, Kastritis PL, Bonvin AM, Vangone AJB. PRODIGY: a web server for predicting the binding affinity of protein–protein complexes. Bioinformatics 2016;32(23):3676-8.
52. Saha S, Raghava GPS, editors. BcePred: prediction of continuous B-cell epitopes in antigenic sequences using physico-chemical properties. International Conference on Artificial Immune Systems; 2004: Springer.
53. Ansari HR, Raghava GP. Identification of conformational B-cell Epitopes in an antigen from its primary sequence. Immunome Res 2010;6:6.
54. Kim Y, Ponomarenko J, Zhu Z, Tamang D, Wang P, Greenbaum J, et al. Immune epitope database analysis resource. Nucleic Acids Res 2012;40(Web server issue): W525-W30.
55. Zuker M, Stiegler P. Optimal computer folding of large RNA sequences using thermodynamics and auxiliary information. Nucleic Acids Res 1981;9(1):133-48.
56. Umu SU, Gardner PP. A comprehensive benchmark of RNA–RNA interaction prediction tools for all domains of life. Bioinformatics 2017;33(7):988-96.
57. Zuker M. Mfold web server for nucleic acid folding and hybridization prediction. Nucleic Acids Res 2003;31(13): 3406-15.

58. Schnupf P, Sansonetti PJ. Shigella pathogenesis: new insights through advanced methodologies. Microbiol Spectr 2019;7(2).

59. Puzari M, Sharma M, Chetia P. Emergence of antibiotic resistant Shigella species: a matter of concern. J Infect Public Health 2018;11(4):451-4.

60. Jennison AV, Verma NK. Shigella flexneri infection: pathogenesis and vaccine development. FEMS Microbiol Rev 2004;28(1):43-58.

61. Levine MM, Kotloff KL, Barry EM, Pasetti MF, Sztein MB. Clinical trials of Shigella vaccines: two steps forward and one step back on a long, hard road. Nat Rev Microbiol 2007;5(7):540-53.

62. Levine MM. Immunogenicity and efficacy of oral vaccines in developing countries: lessons from a live cholera vaccine. BMC Biol 2010;8(1):129.

63. Blanco J, Blanco M, Garabal JL, González EA. Enterotoxins, colonization factors and serotypes of enterotoxigenic Escherichia colifrom humans and animals. Microbiologia 1991;7(2):57-73.

64. Espina M, Olive AJ, Kenjale R, Moore DS, Ausar SF, Kaminski RW, et al. IpaD localizes to the tip of the type III secretion system needle of Shigella flexneri. Infect Immun 2006;74(8):4391-400.

65. Taheri M, Nazarian S, Ebrahimi F, Bakhshi M, Fathi J. Immunogenic evaluation of recombinant chimeric protein containing EspA-Stx2b-Intimin against E. coli O157 H7. Scientific J Kurdistan Univ Med Sci 2018;22 (6):49-62.

66. Gupta P, Singh MK, Singh Y, Gautam V, Kumar S, Kumar O, et al. Recombinant Shiga toxin B subunit elicits protection against Shiga toxin via mixed Th type immune response in mice. Vaccine 2011;29(45):8094-100.

67. Theri M, Nazarian S, Ebrahimi F, Fathi J. Immunization evaluation of type III secretion system recombinant antigens and Shiga like toxin binding subunit of E. coli O157: H7. J Babol Univ Med Sci 2018;20(7):47-54.

68. Yang H, Duan G, Zhu J, Lv R, Xi Y, Zhang W, et al. The AcrAB-TolC pump is involved in multidrug resistance in clinical Shigella flexneri isolates. Microb Drug Resist 2008;14(4):245-9.

69. Kordbacheh E, Nazarian S, Amerian M. In Silico analysis of a multi-subunit immunogen, targeting virulence factors of enterohemorrhagic Escherichia coli. J Applied Biotechnology Reports 2017;4(2):593-602.

70. Felegary A, Nazarian S, Kordbacheh E, Fathi J, Minae ME. An approach to chimeric subunit immunogen provides efficient protection against toxicity, type III and type v secretion systems of Shigella. Int Immuno-pharmacol 2021;100:108132.